

Accepted Manuscript

Title: Caffeine as base analogue of adenine or guanine: A theoretical study

Author: <ce:author id="aut0005"> Ali Ebrahimi<ce:author id="aut0010"> Mostafa Habibi-Khorassani<ce:author id="aut0015"> Farideh Badichi Akher<ce:author id="aut0020"> Abdolkarim Farrokhzadeh<ce:author id="aut0025"> Pouya Karimi



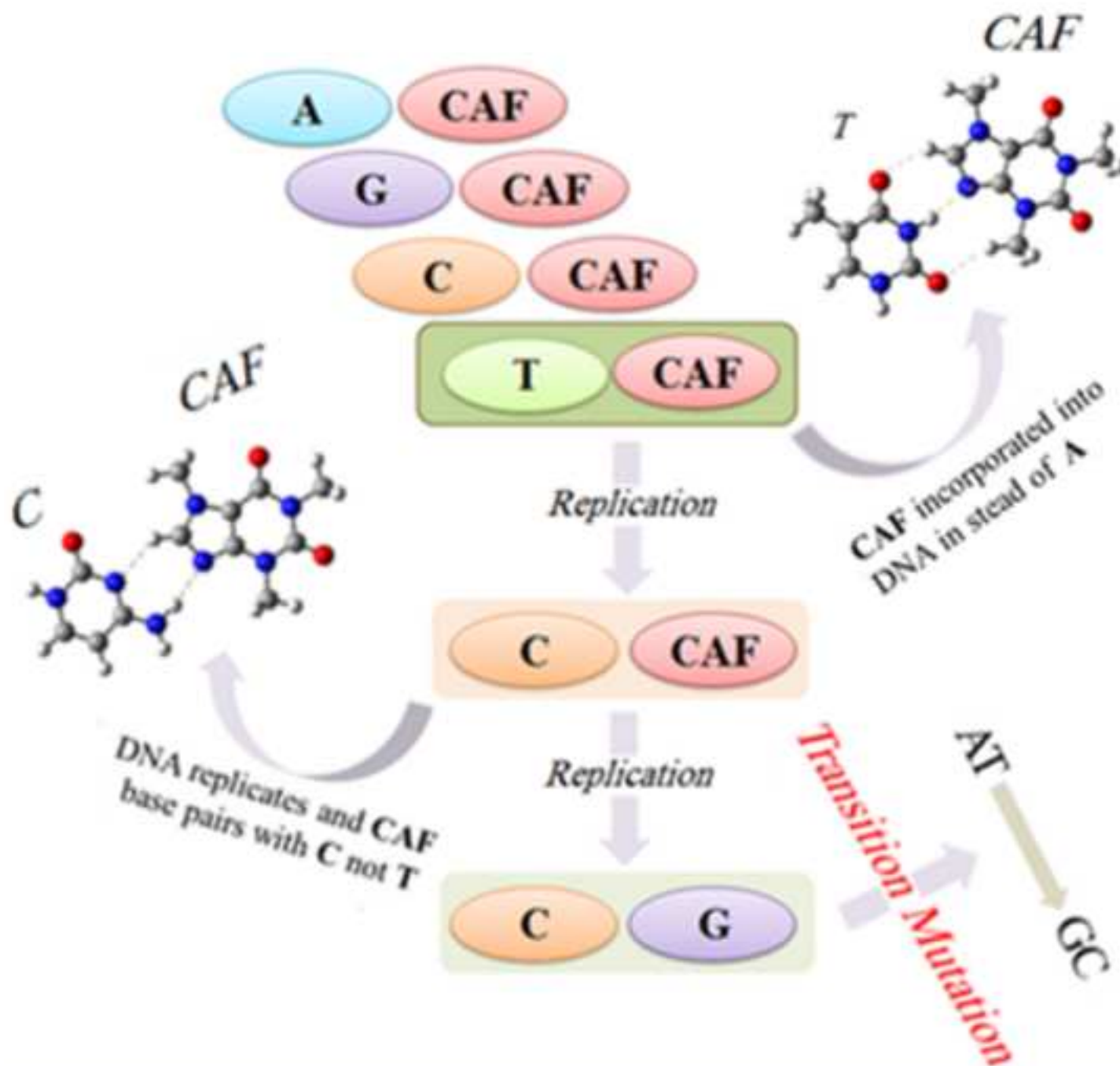
PII: S1093-3263(13)00046-6
DOI: <http://dx.doi.org/doi:10.1016/j.jmgm.2013.02.012>
Reference: JMG 6266

To appear in: *Journal of Molecular Graphics and Modelling*

Received date: 1-7-2012
Revised date: 27-2-2013
Accepted date: 28-2-2013

Please cite this article as: A. Ebrahimi, M. Habibi-Khorassani, F.B. Akher, A. Farrokhzadeh, P. Karimi, Caffeine as base analogue of adenine or guanine: a theoretical study, *Journal of Molecular Graphics and Modelling* (2013), <http://dx.doi.org/10.1016/j.jmgm.2013.02.012>

This is a PDF file of an unedited manuscript that has been accepted for publication. As a service to our customers we are providing this early version of the manuscript. The manuscript will undergo copyediting, typesetting, and review of the resulting proof before it is published in its final form. Please note that during the production process errors may be discovered which could affect the content, and all legal disclaimers that apply to the journal pertain.



- QM calculations are important in better understanding the DNA interactions.
- Caffeine interactions with DNA bases have evaluated.
- Caffeine has weak mutagenic effects.
- Comparison between **CAF-T** and **CAF-C** help in understanding the mutagenic effect.

Caffeine as base analogue of adenine or guanine: a theoretical study

Ali Ebrahimi, Mostafa Habibi-Khorassani, Farideh Badichi Akher*, Abdolkarim Farrokhzadeh and Pouya Karimi

Department of Chemistry, Computational Quantum Chemistry Laboratory, University of Sistan & Baluchestan, P.O. Box 98135-674, Zahedan, Iran

faridehbadichi@yahoo.com (F.Badichi Akher)

Abstract

The results of quantum mechanical calculations, including binding energies and results of the population analysis show that the **GC** and **AT** base pair complexes are more stable than the **CAF-X** ones (where **CAF** is caffeine and **X** = adenine (**A**), thymine (**T**), cytosine (**C**) and guanine (**G**)). Structural similarity between the **CAF** molecule and purine bases (**G** and **A**) provides the possibility of incorporation of the **CAF** molecule into the DNA macromolecule. By comparing the **CAF-A** and **CAF-T** complexes with the **AT** base pair, and the **CAF-G** and **CAF-C** complexes with the **GC** base pair, it was found that the formation of the **CAF-T** complex is more probable than the other complexes. Thus, the **CAF** molecule acts as an analogue base of **A** and can be incorporated into the DNA macromolecule and paired with **T** and **C** in normal and rare state, respectively. Indeed, the results show that formation of the **CAF-C** complex is less probable than the **CAF-T** one and an **AT** to **GC** conversion is rarely occurred in the next DNA replication, so the **CAF** molecule may be considered as a weak mutagenic compound. To

* Corresponding author E-mail: faridehbadichi@yahoo.com (F.Badichi Akher)
Fax: +98-541-2446565

examine solvent effect, the binding energies have been calculated in solvent for the most important structures of the **CAF-G**, **CAF-T**, **CAF-A** and **CAF-C** complexes. The results in solvent are in agreement with those in the gas phase.

Keywords: caffeine; guanine; cytosine; hydrogen bond; transition mutation

Introduction

Pairing errors are known to be responsible for DNA damage which can occur within the DNA helix and cause many human diseases including cancer. The DNA of all living organisms is always subject to different types of damage [1,2]. The direct misincorporation of DNA lesions such as DNA adducts (addition products), modified nucleobases and base analogues, during genetic replication are the frequent DNA damages that are not always effectively identified and repaired by the enzymatic repair systems [3,4].

Several theoretical studies have been performed on the complexes of nucleobases and DNA lesions [5,6,7]. Shyi-Long Lee and coworkers investigated all positions of the interactions between N^{2,3}-ethenoguanine (N^{2,3}- ϵ G) adduct and the DNA nucleotides [6]. They considered several conformations of the ϵ G-A, ϵ G-T, ϵ G-G, and ϵ G-C complexes in connection with different types of hydrogen-bond interactions in terms of the modes of misincorporation. Relative binding energies of complexes in the gas and aqueous phases were compared with reported interaction energies of the GC base pair in Watson–Crick conformation. The computed reaction enthalpies for the N^{2,3}-ethenoguanine adduct and DNA bases at the M06/6-31+G* level indicated that guanine and thymine are most favorable for mispairing with the N^{2,3}-ethenoguanine adduct.

In order to obtain valuable information about misincorporation of the DNA nucleotides into the DNA adducts, the interactions of 1,N⁶-ethenoadenine adducts (**εA**) and 1,N⁶-ethanoadenine adducts (**EA**) with the thymine molecule have been theoretically studied by Venkatesan Srinivasadesikan et al [7]. The geometrical parameters, energetic properties, and binding energies of different conformers of above mentioned complexes have been compared with the **AT** base pair in Watson–Crick conformation. The binding energies for the most stable adenine adduct-thymine complexes (**εA-T**, **EA-T**) are higher than the **AT** base pair. Thus, the DNA adducts can be mispaired with normal DNA bases and lead to the danger of carcinogenesis.

All DNA mispairings in both cis and trans configurations (with respect to glycoside bonds) have been investigated by the molecular electrostatic potentials (MEPs), adiabatic dissociation energy, vertical dissociation energy, and other characteristics [8]. The most stable complex corresponds to the **CG** base pair. Furthermore, the MEP analysis determines unique affinity between **A** and **T** as well as between **G** and **C**.

Methylxanthines are structurally similar to the nucleic acid components and are considered as the purine alkaloids. Therefore, they can be incorporated into the DNA macromolecule because of their purine features [8].

Caffeine (**CAF**) as a methylxanthine is found in tea, coffee, and other beverages and included in many medicines [9,10]; so various doses of the **CAF** molecule are consumed by a great number of people [11]. Also, the stimulating effects of caffeinated beverages can be a reason for the extensive consumption of the **CAF** molecule [12]. It is noted that the **CAF** molecule makes health risks in the children, pregnant and some patients [13,14]. Also, it is a purine alkaloid [15,16] and a base analogue of **A**. Thus, the **CAF** molecule has a mutagenic effect [11,17,18]

and can sometimes paired with **T** instead of **A** in normal state, and with **C** in its rare state and causes a **AT**→**GC** transition mutation (see Scheme 1).

In the present work, interaction of the **CAF** molecule with the DNA bases have been investigated by considering different conformers of the **CAF-X** (where **X** = **A**, **T**, **C** and **G**) complexes. The most important conformers of the **CAF-X** complexes have been investigated by energetics calculations and population analyses to clarify the action of the **CAF** molecule as base analogue of **A**. Comparison of the **CAF-A** and **CAF-T** complexes with the **AT** base pair and the **CAF-G** and **CAF-C** complexes with the **GC** base pair can be helpful for this purpose. Furthermore, the weak mutagenic effect of the **CAF** molecule was investigated by comparison between the **CAF-T** and **CAF-C** complexes. In addition, we explored the role of solvent on the binding energies of the most important conformations of the **CAF-X** complexes.

Computational methods

Geometries of the monomers and complexes were optimized by the Gaussian09 [19] program package using a hybrid density functional (B3LYP) [20] method and the 6-311++G(d,p) basis set. Single-point calculations were carried out using the MPWPW91 [21] method in conjunction with the 6-311++G(d,p) basis set and the PBEKCIS [22] method in conjunction with the 6-311++G(d,p) and AUG-cc-pVDZ basis sets for the **AT** and **GC** base pairs. The interaction energies were corrected for the basis set superposition error (BSSE) using the counterpoise method of the Boys and Bernardi [23]. The basis set superposition error (BSSE) correction was carried out with B3LYP method in conjunction with the 6-311++G(d,p) basis set. Vibrational

frequency analysis was carried out on optimized structures at the B3LYP/6-311++G(d,p) level of theory.

The topological properties of electron charge density were calculated by the atoms in molecules (AIM) method [24] using the AIM2000 program package [25] at the B3LYP/6-311++G(d,p) level of theory. The natural bond orbital (NBO) analysis [26] was performed at the B3LYP/6-311++G(d,p) level by the NBO3.1 [27] program. Moreover, the atomic charge distributions were calculated for the complexes and constituent units using the ChelpG method [28] on the structures optimized at the above mentioned level.

To evaluate interaction energies in solvated environment with water as solvent, based on optimized gas phase geometries, energy calculations were performed using the self-consistent reaction field (SCRF) method [29] by the integration equation formalism polarizable continuum model (IEF-PCM) [30] at the B3LYP/6-311++G** level for the most important conformations of the **CAF-X** (where **X** = **A**, **T**, **C** and **G**) complexes.

Results and discussion

The atom numbering and charge on the atoms of **G**, **A**, **C**, **T** and **CAF** are shown in Figure 1. Six different conformers (**a**, **b**, **c**, **d**, **e** and **f**) for each type of the CAF-X complexes have been considered. The binding energies (ΔE) of these conformers and the **AT**, **GC** base pairs calculated at the B3LYP/6-311G(d,p) level of theory are given in Table 1. The ΔE values lie in the ranges of -8.30 – -11.92, -5.25 – -9.25, -5.93 – -8.55 and -1.00 – -6.41 kcal mol⁻¹ for the complexes of **CAF** with **G**, **C**, **T** and **A**, respectively. According to the ΔE values, stability of the complexes decreases as **GC** > **AT** > **CAF-G** > **CAF-C** > **CAF-T** > **CAF-A**.

To obtain a more accurate interaction energy of the complexes, we have also carried out single point calculations at the MPWPW91/6-311++G(d,p), PBEKCIS/6-311++G(d,p) and PBEKCIS/AUG-cc-pVDZ levels on the geometries optimized at the B3LYP/6-311++G(d,p) level of theory for the **AT** and **GC** base pairs. Among these, the B3LYP/6-311++G(d,p) level provides geometries and interaction energies in agreement with high accurate CCSD(T) calculations [31]. Therefore, we only report on the B3LYP results throughout the text.

The optimized geometries of the most important conformers of the **CAF-G** complexes obtained at the B3LYP/6-311++G(d,p) level of theory, intermolecular H-bond distances, H-bond angles and ChelpG charges are gathered in Figure 2. Here in, three H-bonds are expected between **CAF** and **G** (with exception of the conformer **e**). The H-bond lengths lie in the range of 1.94-2.69 Å. A good linear correlation is found between the ΔE values and the CH...O H-bond lengths for the **CAF-G** conformers (with exception of the conformer **e**). As can be seen in Figure 3, increase in the ΔE values is accompanied by decrease in the CH...O H-bond lengths.

The H-bond angles are in the range of 142.15 – 170.92°. It may be expected that the deviation of the H-bond angles from 180° decrease by increasing the ΔE values of the complexes. However, because of geometrical restrictions in multi H-bonded complexes there is not any meaningful relationship between the stability of the complexes and the H-bond angles.

The H1 atom involved in the N1H1...O6 H-bond in the conformer **a** has more positive charge relative to the conformer **d** after complexation. The H21 atom involved in the N2H21...O6 H-bond has lower positive charge in both the conformers **a** and **d**, while its charge in the conformer **a** is more positive than the conformer **d**. In addition, the H atom involved in the CH...O H-bond has more positive charge in the conformer **a** relative to the conformer **d**. Thus, higher

electrostatic interaction can contribute to the more stability of the complex **a**. By a similar discussion, higher stability of the conformer **b** relative to the conformer **c** can be attributed to electrostatic interactions. The positive charges of the H1 and H21 atoms involved in the N1H1...N9 and N2H21...N9 H-bonds decrease during complexation in the conformer **f**. Also, the positive charge of the H1 atom involved in the N1H1...N9 H-bond decrease during complexation in the conformer **e**. Since, the H8 atom is more positive than H31 in the **CAF** molecule, the H8 atom in the conformer **e** is more susceptible than H31 in the conformer **f** to the formation of the CH...O H-bond.

The optimized structures of the most important conformers of the **CAF-T** complexes, intermolecular H-bond distances, H-bond angles and the ChelpG charges are given in Figure 4. Three H-bonds are observed for all optimized **CAF-T** complexes. A common feature of the two conformers **a** and **b**, **c** and **d**, **e** and **f** is the presence of an identical central H-bond. There are one NH...N and two CH...O H-bonds in the conformers **a** and **b**. One NH...O and two CH...O H-bonds are observed for other conformers.

The H-bond lengths in the **CAF-T** complexes lie in the range of 1.83– 2.81 Å. The bond length of the central H-bond in the conformer **a** (NH...N, 1.94 Å), **c** (NH...O, 1.83 Å) and **e** (NH...O, 1.85 Å), is same with that is observed in **b**, **d**, and **f**, respectively. The NH...N bond length in **a** and **b** is higher than other conformers. The H-bond donors of the CH...O H-bonds in the conformers **a** and **b** are sp^3 (-CH₃) and sp^2 (-CH in five-membered ring) hybridized carbon atoms, respectively. However, these H-bond donors correspond to sp^3 (-CH₃) hybridized carbon atoms in other conformers. As a rule, acidity of the CH group, and its hydrogen bond donor nature, increments by changing from the sp^3 over sp^2 to sp hybridized C atom and also by adjacent electron withdrawing atoms [32,33,34]. Thus, the CH group of the five-membered ring

in the conformer **a** and **b** is more susceptible to the CH \cdots O H-bond formation relative to the CH₃ group in the other conformer. It should be noted that in these conformers a good linear correlation isn't found between the ΔE values and the CH \cdots O H-bond lengths.

The H-bond angles lie in the range of 134.95-177.70°. Similar to the complexes **CAF-G**, the deviation of the H-bond angles from the 180° approximately increments by increasing stability of the complexes.

The positive charges of the H atoms involved in the C-H \cdots O bands of the conformers **a** and **b** increase during complexation, while a reverse change is observed for the other conformers. The maximum total charges (in brackets) on **CAF** and **T** correspond to the conformers **a** and **b** (0.1e) and the minimum values correspond to the conformers **e** and **f** (0.02e). Therefore, stability of the conformers increments by increasing the strength of the electrostatic interactions. These are in agreement with the energy data.

The optimized geometries of the most important conformers of the **CAF-A** complexes, H-bond distances, H-bond angles and the ChelpG charges are shown in Figure 5. The interaction between **CAF** and **A** includes two H-bonds. The H-bond lengths lie in the range of 1.95-2.84 Å, where the minimum/maximum bond length corresponds to the NH \cdots O/CH \cdots N H-bond in the conformer **a/f**. It is also noteworthy that the complexation is accompanied by the strong H-bonds NH \cdots O or NH \cdots N in the most stable conformers (**a**, **b** and **c**) while it is accompanied by the weak H-bonds CH \cdots N and CH \cdots O in the other conformers.

As can be seen in Figure 3, a good linear correlation ($R = 0.99$) is found between the ΔE values and CH \cdots N H-bond lengths for the **CAF-A** conformers (with exception of the conformer **e**). This shows that the CH \cdots N H-bond lengths decreases (become shorter) with increasing binding

energies of the conformers. The H-bond angles in the **CAF-A** conformers change in the range 174.49-145.27° and stability of these conformers increments by decreasing the deviation of the H-bond angle from 180°.

The H atoms involved in H-bonds of the conformer **a** (the most stable conformer) have more positive charge than the other **CAF-A** conformers after complexation. On the other hand, the positive charges on the H atoms involved in H-bonds of the conformer **f** are lower than the other **CAF-A** conformers. Therefore, more stability of the conformer **a** may correspond to the strong electrostatic interaction. The results are consistent with energy data.

The optimized geometries of the most important conformers of the **CAF-C** complexes, H-bond distances, H-bond angles and ChelpG charges are shown in Figure 6. Herein, two H-bonds are observed between **CAF** and **C**. The H-bond lengths lie in the range of 1.92-2.50 Å. There is correlation between the CH...N H-bond lengths and the ΔE values for the **CAF-C** conformers (with exception of the conformer **f**). The linear correlation coefficient for this dependence amounts to 0.99 (see Figure 3).

The H-bond angles change in the range 171.95-139.16°. H-bonds angle deviations from 180° in the **CAF-C** conformers decrements by increasing the stability of the conformers (with the exception of **a**).

The positive charge on the H atoms involved in the NH...N and CH...N H-bonds of the conformer **a** are lower than **f** after complexation. On the other hand, the energy data show that the conformer **a** is more stable than the other **CAF-C** conformers.

The H8 atom is more positive than the H31 atom on the base of ChelpG charges in the **CAF** molecule. Therefore, the H8 atom in the conformer **a** is more susceptible to H-bond formation

(CH...N) relative to the conformer **f**. This is in agreement with the results mentioned above. The H atoms involved in the NH...O and CH...N H-bonds of the conformer **b** gain more positive charge in comparison with the H atoms involved in the H-bonds of the conformer **e**. Thus, the effect of electrostatic interaction on the stability of the conformer **b** may be very important. The positive ChelpG charge on the H atom involved in the NH...O H-bond of the conformer **c** is lower than those involved in the NH...O H-bonds of the conformers **d** and **e**. The H atom involved in the CH...N H-bond of the conformer **c** gain more positive charge than those involved in the CH...N H-bonds of the conformers **d** and **e**. Thus, effect of electrostatic interaction on the CH...N H-bond in the conformer **c** is stronger than **d** and **e**.

AIM and NBO analyses

A way to characterize the hydrogen bonds with different strengths is AIM analysis which has successfully been applied in a wide variety of molecular complexes [35,36]. The electron charge density (ρ) values calculated at the H-bond critical points (HBCP) of complexes lie in the range of 4.0×10^{-3} - 30.0×10^{-3} e/au³ (See Table 2).

The $\sum \rho_{\text{HBCP}}$ values lie in the range of 42.1×10^{-3} - 52.7×10^{-3} e/au³ in the **CAF-G** conformers. The highest/lowest $\sum \rho_{\text{HBCP}}$ value corresponds to the conformer **a/f**. Herein, the ΔE values increment by increasing $\sum \rho_{\text{HBCP}}$.

In the **CAF-T** conformers, among three strong H-bonds, the N3H3...N9 bond in the conformers **a** and **b**, the N3H3...O6 bond in the conformers **c** and **d**, and the N3H3...O2 bond in the conformers **e** and **f**, the highest/lowest value of ρ corresponds to the N3H3...N9/N3H3...O2 H-bond. Also, two weak CH...O bonds are observed in each conformer which the maximum ρ_{HBCP}

value is observed for the C8H8...O4 and C8H8...O2 BCPs of the conformers **a** and **b**, respectively. The $\sum\rho_{\text{HBCP}}$ values in the **CAF-T** conformers lie in the range of 41.9×10^{-3} - 50.9×10^{-3} e/au³. The highest values correspond to the conformers **a** (50.9×10^{-3}) and **b** (50.6×10^{-3}) and the lowest values correspond to the conformers **e** (41.9×10^{-3}) and **f** (42.0×10^{-3}). Thus, stability of the conformers **a** and **b** increments by increasing the $\sum\rho_{\text{HBCP}}$ values.

There are two H-bonds in the conformers **a**, **b** and **c** of the **CAF-A** complex, one strong NH...O (or NH...N) H-bond and one weak CH...N H-bond, while two weak H-bonds (CH...N or CH...O) are observed for other conformers. The more stability of the conformers **a**, **b** and **c** relative to the other conformers may be attributed to the above mentioned interactions.

The highest/lowest $\sum\rho_{\text{HBCP}}$ value corresponds to the conformer **a/f**, and the difference between $\sum\rho_{\text{HBCP}}$ values of the conformers **b** and **c** is negligible.

The highest $\sum\rho_{\text{HBCP}}$ value corresponds to the conformer **a** in the **CAF-C** complex. Some individual H-bonds of the conformer **f** are stronger than **a**, but the $\sum\rho_{\text{HBCP}}$ value in the conformer **a** (more stable) is higher than **f**. Comparison between the conformers **b** and **e** (or **c** and **d**) lead to a similar discussion mentioned for **a** and **f** which the more stable conformer (**b** or **c**) has a higher $\sum\rho_{\text{HBCP}}$ value.

To explore other features of individual H-bonds, the NBO analysis has also been carried out at the B3LYP/6-311++G(d,p) level of theory. The donor-acceptor interaction energies (E^2) are given in Table 3.

In these multiple H-bond complexes, orientation of functional groups involved in each H-bond is affected by corresponding orientations in other complexes. The establishment of appropriate orientation for donor-acceptor interactions in the NH...N H-bond with one lone pairs, is easier

than the $\text{NH}\cdots\text{O}$ H-bond with two lone pairs. Therefore, donor-acceptor interaction of the $\text{NH}\cdots\text{N}$ H-bond is abnormally higher than the $\text{NH}\cdots\text{O}$ H-bond, and reasonable relationships are not observed between ΣE^2 and the binding energy values for **CAF-G**, **CAF-A** and **CAF-C** conformers, but the binding energies increment by increasing ΣE^2 values correspond to each of the **CAF-T** conformers. However, these values do not include the electrostatic contributions to the strength of hydrogen bond.

According to the energy data presented in Table 1, we can affirm that the stability of the **AT** and **GC** base pairs is more than the **CAF-A**, **CAF-T**, **CAF-G** and **CAF-C** complexes. Thus, the **A** base will pair with the **T** base and **G** with **C**, in the ideal case. However, the structural similarity between the **CAF** molecule and purine bases (**A** and **G**) may be reason for incorporation of the **CAF** molecule into a growing DNA chain. Furthermore, the **CAF** molecule as base analogue of the **A** or **G** must be investigated.

The difference between binding energy of the **AT** base pair with the **CAF-A** and **CAF-T** complexes, and the **GC** base pair with the **CAF-G** and **CAF-C** complexes was considered. The lowest value corresponds to the difference between binding energy of the **AT** base pair and the **CAF-T** complex. Also, the results of population analyses in the Table 2 and 3 show that the maximum values of $\Sigma \rho_{\text{HBCP}}$ and ΣE^2 values correspond to the **AT** and **GC** base pairs. The lowest difference between the $\Sigma \rho_{\text{HBCP}}$ (and ΣE^2) values corresponds to the pair **CAF-T** and **AT**. Consequently, **CAF** can be considered as a base analogue of **A**.

To clarify the weak mutagenic effect of the **CAF** molecule, the **CAF-T** complex compared with the **CAF-C** complex. The results show that the $\Sigma \rho_{\text{HBCP}}$ and ΣE^2 values of the **CAF-T** complex are more than the **CAF-C** complex. In the **CAF-T** complex, the deviation of the H-bond angles

from 180° is lower than the **CAF-C** complex. Also, the charge transfer in the **CAF-T** complex is more than the **CAF-C** complex. Thus, formation of the **CAF-C** complex is less probable than the **CAF-T** complex and conversion of the **AT** to **GC** base pair rarely occurs in the next DNA replication. For this reason, the **CAF** molecule can not be considered as a strong mutagenic. As can be seen from table 1 the effect of solvent on the binding energies of the most stable conformations of the **CAF-A**, **CAF-T**, **CAF-G** and **CAF-C** complexes investigated in solvated environment with water as solvent, based on optimized gas phase geometries. Compared to the gas phase, the binding energies of the complexes decrease, but the trend is preserved. The results are in agreement with the gas phase conclusion.

Conclusions

In order to investigate the action of the **CAF** molecule as base analogue of **A** and its weak mutagenic effect, interactions of the **CAF** molecule with each of the DNA bases have been considered. The ΔE , $\sum E^2$ and $\sum \rho$ values of the **AT** and **GC** base pairs are higher than the most stable conformations of the **CAF-A**, **CAF-T**, **CAF-G** and **CAF-C** complexes. Comparison between the binding energies of the **CAF-A** and **CAF-T** complexes with the **AT** base pair, and **CAF-G** and **CAF-C** complexes with the **GC** base pair, indicates that the lowest difference exists between the **CAF-T** complex and the **AT** base pair. Thus the **CAF** molecule may be considered as a base analogue of **A**. Normally, the **CAF** molecule that resembles **A**, may be paired with **T** and incorporates into DNA during DNA replication. In a rare state, the **CAF** molecule may be paired with **C** and lead to a transition mutation (**AT**→**GC**). The results show that the $\sum E^2$, $\sum \rho$, number of H-bonds and charge transfer are higher for the more stable **CAF-T** complex in

comparison with the **CAF-C** complex. Thus, formation of the **CAF-C** complex is less probable in comparison with the **CAF-T** complex and the **AT**→**GC** conversion rarely occurs in the next DNA replication. Thus, the **CAF** molecule can not be considered as strong mutagenic agent. The results of calculations in solvent environment are in accord with the gas phase ones.

Acknowledgment

We thank the university of Sistan & Baluchestan for financial supports and Computational Quantum Chemistry Laboratory for computational facilities.

References

-
- [1] J.C Lin, R.R. P. Singh and D.L. Cox, Theoretical Study of DNA Damage Recognition via Electron Transfer from the [4Fe-4S] Complex of MutY. *Biophysical Journal* 95 (7) 3259-3268.
 - [2] M.S. Cooke, M.D. Evans, M.Dizdaroglu and J. Lunec.. Oxidative DNA damage: mechanisms, mutation, and disease. *FASEB J.* 17 (2003) 1195–1214.
 - [3] J. Berashevich and T. Chakraborty, Thermodynamics of GA mispairs in DNA: Continuum electrostatic model. *The journal of chemical physics.* 130 (2009) 015101-8.
 - [4] G. Marra and P. Schär, Recognition of DNA alterations by the mismatch repair system. *Biochem. J.* 338 (1999) 1–13.

-
- [5] P.K. Sahu, C.W Kuo, and S.L Lee, Interaction of adenine adducts with thymine: acomputational study. *J. Phys. Chem. B*.111 (2007) 2991-2998.
- [6] V. Srinivasadesikan, P.K. Sahu, and S.L Lee, Model calculations for the misincorporation of nucleotides opposite five-membered exocyclic DNA adduct: N^{2,3}-ethenoguanine. *J. Phys. Chem. B*.115 (2011) 10537–10546.
- [7] I. Otero-Navas and J. M. Seminario, Molecular electrostatic potentials of DNA base–base pairing and mispairing. *J. Mol. Model*18 (2012) 91-101.
- [8] S.M. Tarka, J.J. Hurst and W.J. Hurst, Caffeine. CRC Press: New York, 1998.
- [9] H. Terada and Y. Sakabe, performance liquid chromatographic determination of theobromine, theophylline and caffeine in food products. *J. Chromatogr.* 291 (1984) 453-459.
- [10] T. Kumazawaa, H. Senob, X.P Leea, A. Ishiib, K.W Suzukib, K. Satoa and O. Suzukib, Extraction of methylxanthines from human body fluids by solid-phase microextraction. *Analytica Chimica Acta.* 387 (1999) 53–60.
- [11] T. Khursheed, M.Y.K Ansari and D. Shahab, Studies on the effect of caffeine on growth and yield parameters in *Helianthus annuus* L. variety Modern. *Biology and Medicine.* 1 (2009) 56-60.
- [12] S.R. Waldvogel, Caffeine–A Drug with a Surprise. *Angew. Chem. Int. Ed.* 42 (2003) 604-605.
- [13] H. İcen and M. Gürü, Extraction of caffeine from tea stalk and fiber wastes using supercritical carbon dioxide. *J. Supercrit. Fluids.* 50 (2009) 225–228.
- [14] A.M.M.N. El-Din and S.H. Abu-Raiia, Technological study on the production of tea. *Egypt. J. Food Sci.* 23 (1995) 241–245.

-
- [15] M. Melnik, Binuclear caffeine adducts of Cu(II)acetate and Cu(II) chloracetates with unusually high antiferromagnetic interaction. *Journal of inorganic and nuclear chemistry*. 43 (1981) 3035-3038.
- [16] S.A. Shaker, Y. Farina, S. Mahmmoud and M. Eskender, Preparation and study of mixed ligand complexes of caffeine and cyanate with some metal ions. *Australian Journal of Basic and Applied Sciences*. 3(2009) 3337-3340.
- [17] E. Maxim, G. Capraru and F.M. Axente, Estimation of citogenetic effects on caffeine treatment in dill root meristems. *Secțiunea Genetică și Biologie Moleculară, TOM X*, 2009.
- [18] T. McKee and J.R. McKee, *Biochemistry*. McGraw-Hill, New York, 2003.
- [19] M.J. Frisch and et al., *Gaussian 09, Revision A.02*; Gaussian Inc. Wallingford CT, 2009.
- [20] A.D. Becke, Density-functional thermochemistry. III. The role of exact exchange. *J. Chem. Phys.* 98 (1993) 5648 -5652.
- [21] C. Adamo and V. Barone, Exchange functionals with improved long-range behavior and adiabatic connection methods without adjustable parameters: the mPW and mPW1PW models. *J. Chem. Phys.* 108 (1998) 664-675.
- [22] Y. Zhao and D.G. Truhlar, Benchmark databases for nonbonded interactions and their use to test density functional theory. *J. Chem. Theory Comput.* 1 (2005) 415-432.
- [23] S.F. Boys and F. Bernardi, Calculation of small molecular interactions by differences of separate total energies - some procedures with reduced errors. *Mol. Phys.* 19 (1970) 553-566.
- [24] R.F.W. Bader, *Atoms in molecules: a quantum theory*. Oxford University Press, Oxford, 1990.
- [25] F.W. BieglerKönig, J. Schönbohm and D. Bayles, AIM2000 - A program to analyze and visualize atoms in molecules. *J. Comput. Chem.* 22 (2001) 545-559.

-
- [26] A.E. Reed, L.A. Curtiss and F. Weinhold, Intermolecular interactions from a natural bond orbital, donor-acceptor viewpoint. *Chem. Rev.* 88 (1988) 899–926.
- [27] E.D. Glendening, A.E. Reed, J.E. Carpenter and F. Weinhold, NBO version 3.1. theoretical chemistry institute. University of Wisconsin, Madison, 1990.
- [28] C.M. Breneman and K.B. Wiberg, Determining atom-centered monopoles from molecular electrostatic potentials - the need for high sampling density in formamide conformational-analysis. *J. Comput. Chem.* 11 (1990) 361–373.
- [29] J. E. Sanhueza and O. Tapia, *J. Mol. Struct. (Theochem)* 89 (1982) 131-146.
- [30] J. Tomasi, B. Mennucci and R. Cammi, Quantum mechanical continuum solvation models. *Chem. Rev.* 105 (2005) 2999–3093.
- [31] P. Hobza, Theoretical studies of hydrogen bonding. *Annu. Rep. Prog. Chem. Sect. C.* 100 (2004) 3–27.
- [32] G. R. Desiraju, The C-H \cdots O hydrogen bond in organic crystals. What is it?. *AccChem Res.* 24 (1991) 290-296.
- [33] T. Steiner, Unrolling the hydrogen bond properties of C-H \cdots O interactions. *ChemCommun.* (1997) 727-734.
- [34] M. Brandl, K. Lindauer, M. Meyer and J. Sühnel, C-H \cdots O and C-H \cdots N interactions in RNA structures. *Theor. Chem. Acc.* 101(1999) 103-113.
- [35] P. Popelier, Characterization of a dihydrogen bond on the basis of the electron density. *J. Phys. Chem. A.* 102 (1998) 1873-1878.
- [36] X. Liang, X. Pu, H. Zhou, N.B. Wong and A. Tian, Keto–enol tautomerization of cyanuric acid in the gas phase and in water and methanol. *Journal of Molecular Structure, THEOCHEM.* 816 (2007) 125–136.

Table 1. The binding energies ($-\Delta E$ in kcal mol⁻¹) corrected for BSSE at B3LYP/6-311++G** level.

B3LYP/6-311++G**				
	CAF-G	CAF-A	CAF-T	CAF-C
a	11.92, 6.42	6.41, 3.70	8.55, 4.93	9.25, 3.98
b	10.67	5.43	8.48	8.93
c	10.04	4.71	7.20	7.17
d	9.20	2.27	7.06	6.37
e	9.14	1.53	5.97	5.65
f	8.30	1.00	5.93	5.25
	B3LYP	MPWPW91	PBECIS	ΔE^{Tot}
GC	25.73, 13.22	31.31	30.19,29.92	26.20
AT	12.66, 7.65	11.38	11.60,11.54	13.80

The bold values correspond to the SCRF calculations. The italicized values have calculated with the AUG-cc-pVDZ basis set. ΔE^{Tot} is sum of $\Delta \text{CCSD(T)}$ and RI/MP2/AUG-cc-pVDZ binding energies ($\Delta \text{CCSD(T)}$ is difference between MP2 and CCSD(T) binding energies calculated at small basis set) which have taken from Ref [43]. **a**, **b**, **c**, **d**, **e** and **f** are six different conformers for each type of the CAF-X complexes.

Table 2. Topological properties of the electron charge density calculated at the bond critical points of the hydrogen bonds for the **AT** and **GC** base pairs and **CAF-X** complexes in au.

	XH...Y	$\rho \times 10^{-3}$	$\Sigma \rho \times 10^{-3}$		XH...Y	$\rho \times 10^{-3}$	$\Sigma \rho \times 10^{-3}$
GC	N4-H42...O6	37.5	96.5	AT	N6-H62...O4	25.8	69.5
	N1-H1...N3	32.6			N3-H3...N1	39.5	
	N2-H21...O2	26.4			C2-H2...O2	4.2	
CAF-G				CAF-T			
a	C7H73...O6	14.3	52.7	a	C8H8...O4	12.4	50.9
	N1H1...O6	23.7			N3H3...N9	30.0	
	N2H21...O6	14.8			C3H31...O2	8.5	
b	N2H21...O2	12.4	47.4	b	C8H8...O2	12.0	50.6
	N1H1...O2	24.7			N3H3...N9	29.8	
	C3H33...O6	10.2			C3H31...O4	8.8	
c	N2H21...O2	12.7	45.7	c	C7H71...O4	11.3	44.6
	N1H1...O2	24.2			N3H3...O6	28.8	
	C1H11...O6	8.8			C1H12...O2	4.5	
d	N2H21...O6	12.6	45.8	d	C1H12...O4	5.4	45.1
	N1H1...O6	24.6			N3H3...O6	29.0	
	C1H12...O6	8.6			C7H71...O2	10.7	
e	N2H21...H31C3	4.0	43.9	e	C3H32...O4	7.8	41.9
	N1H1...N9	22.5			N3H3...O2	28.5	
	C8H8...O6	17.4			C1H11...O2	5.6	
f	N2H21...N9	6.9	42.1	f	C1H13...O4	6.1	42.0
	H1N1...N9	25.8			N3H3...O2	28.4	
	C3H31...O6	9.4			C3H33...O2	7.5	
CAF-A				CAF-C			
a	C7H73...N1	12.8	34.6	a	C8H8...N3	16.2	38.5
	N6H62...O6	21.8			N4H42...N9	22.4	
b	N6H62...O2	21.7	31.7	b	N4H42...O6	22.7	37.5
	C1H13...N1	10.0			C7H73...N3	14.8	
c	N6H62...N9	22.3	31.8	c	N4H42...O2	23.6	35.3
	C3H32...N1	9.6			C3H31...N3	11.6	
d	C8H8...N1	11.1	17.0	d	N4H42...O2	23.5	34.0
	C2H2...N9	6.0			C1H12...N3	10.6	
e	C2H2...O2	9.0	18.2	e	N4H42...O6	23.8	34.3
	C3H33...N1	9.2			C1H12...N3	10.5	
f	C2H2...O6	9.2	14.3	f	N4H42...N9	23.4	34.4
	C1H12...N1	5.1			C3H31...N3	11.0	

a, b, c, d, e and **f** are six different conformers for each type of the **CAF-X** complexes.

Table 3. The donor-acceptor interaction energies (in kcal mol⁻¹) obtained from the NBO analysis at the B3LYP/6-311++G(d,p) level of theory for the **AT** and **GC** base pairs and **CAF-X** complexes.

	XH...Y	E ²	ΣE ²		XH...Y	E ²	ΣE ²
GC	N4-H42...O6	22.16	53.32	AT	N6-H62...O4	11.55	36.66
	N1-H1...N3	18.85			N3-H3...N1	24.79	
	N2-H21...O2	12.31			C2-H2...O2	0.320	
CAF-G				CAF-T			
a	C7H73...O6	2.59	12.30	a	C8H8...O4	2.19	19.65
	N1H1...O6	6.78			N3H3...N9	16.07	
	N2H21...O6	2.93			C3H31...O2	1.39	
b	N2H21...O2	1.95	11.82	b	C8H8...O2	2.12	19.55
	N1H1...O2	7.95			N3H3...N9	15.93	
	C3H33...O6	1.92			C3H31...O4	1.50	
c	N2H21...O2	2.03	10.88	c	C7H71...O4	2.35	12.26
	N1H1...O2	7.39			N3H3...O6	9.38	
	C1H11...O6	1.46			C1H12...O2	0.53	
d	N2H21...O6	1.78	10.70	d	C1H12...O4	0.72	12.27
	N1H1...O6	7.59			N3H3...O6	9.39	
	C1H12...O6	1.33			C7H71...O2	2.16	
e	N1H11...N9	10.01	14.64	e	C3H32...O4	1.28	10.10
	C8H8...O6	4.63			N3H3...O2	8.15	
					C1H11...O2	0.67	
f	N2H21...N9	0.46	14.79	f	C1H13...O4	0.78	10.01
	H1N1...N9	12.96			N3H3...O2	8.04	
	C3H31...O6	1.37			C3H33...O2	1.19	
CAF-A				CAF-C			
a	C7H73...N1	2.54	8.53	a	C8H8...N3	4.24	13.26
	N6H62...O6	5.99			N4H42...N9	9.02	
b	N6H62...O2	6.5	8.53	b	N4H42...O6	6.03	9.87
	C1H13...N1	2.03			C7H73...N3	3.84	
c	N6H62...N9	9.52	11.2	c	N4H42...O2	7.52	10.15
	C3H32...N1	1.68			C3H31...N3	2.63	
d	C8H8...N1	2.81	3.49	d	N4H42...O2	7.57	9.73
	C2H2...N9	0.68			C1H12...N3	2.16	
e	C2H2...O2	1.05	2.74	e	N4H42...O6	8.66	10.67
	C3H33...N1	1.69			C1H12...N3	2.01	
f	C2H2...O6	1.45	1.94	f	N4H42...N9	10.44	12.49
	C1H12...N1	0.49			C3H31...N3	2.05	

a, b, c, d, e and f are six different conformers for each type of the **CAF-X** complexes.

Scheme. 1. Transition mutation (the **AT** base pair changes to the **GC** base pair).

Fig. 1. The structure, atom numbering and charge on the atoms of **G**, **A**, **C**, **T** and **CAF**.

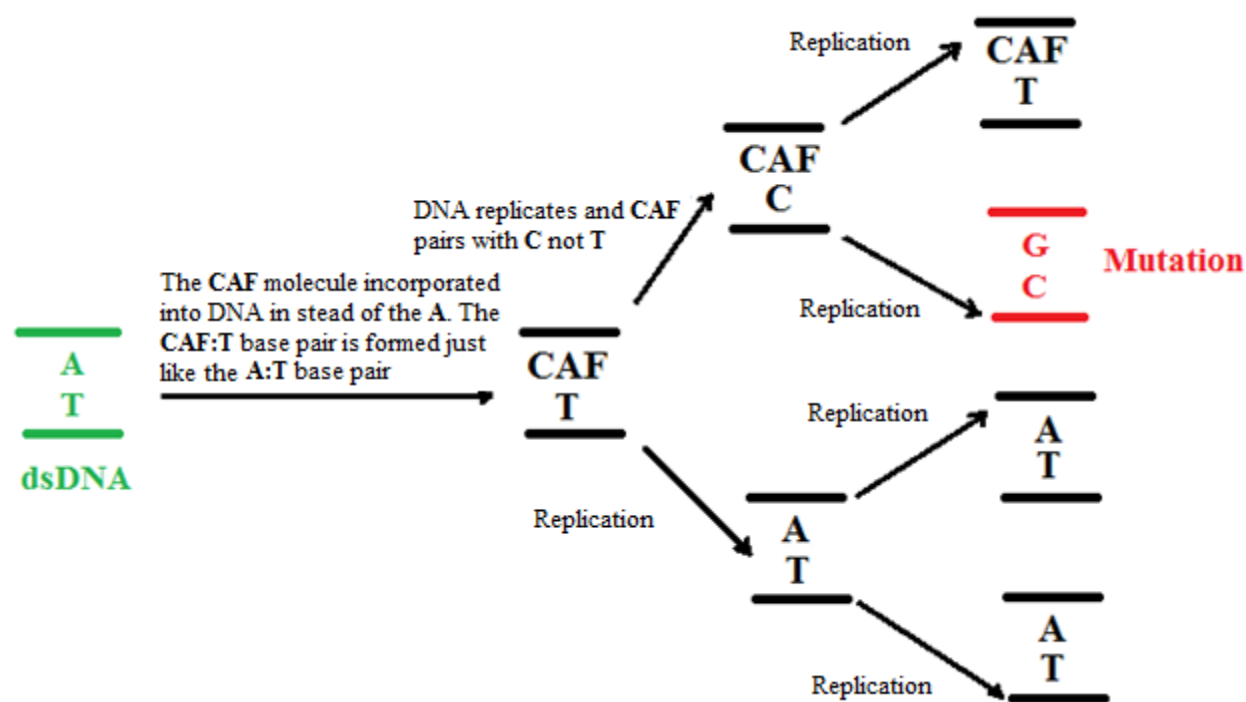
Fig. 2. Six cconformers of the **CAF-G** complex optimized at the B3LYP/6-311++G(d,p) level of theory. Intermolecular H-bond distances (in Å), H-bond angles (in °) and ChelpG charges (in e) have presented. The ChelpG charges calculated for each unit have given in the brakets.

Fig. 3. Correlations between the binding energies and H-bond lengths for conformers of the CAF-X complexes (■: X = **G**, ▲: X = **A** and ●: X = **C**).

Fig. 4. Six conformers of the **CAF-T** complex optimized at the B3LYP/6-311++G(d,p) level of theory. Intermolecular H-bond distances (in Å), H-bond angles (in °) and ChelpG charges (in e) have presented.

Fig. 5. Six conformers of the **CAF-A** complex optimized at the B3LYP/6-311++G(d,p) level of theory. H-bond distances (in Å), the H-bond angles (in °) and ChelpG charges (in e) have presented.

Fig. 6. Six conformers of the **CAF-C** complex optimized at the B3LYP/6-311++G(d,p) level of theory. H-bond distances (in Å), H-bond angles (in °) and ChelpG charges (in e) have presented.



Scheme. 1.

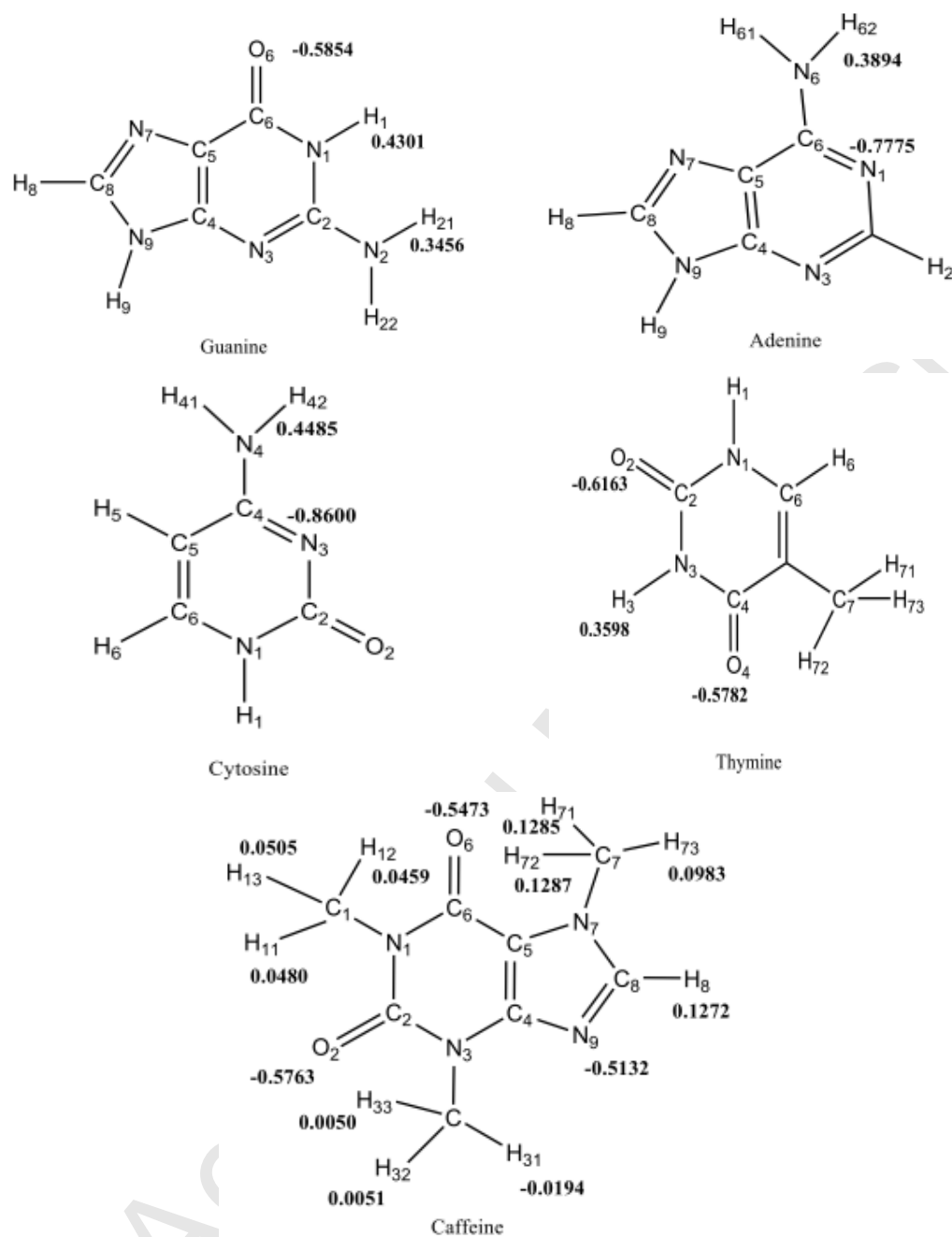


Fig. 1.

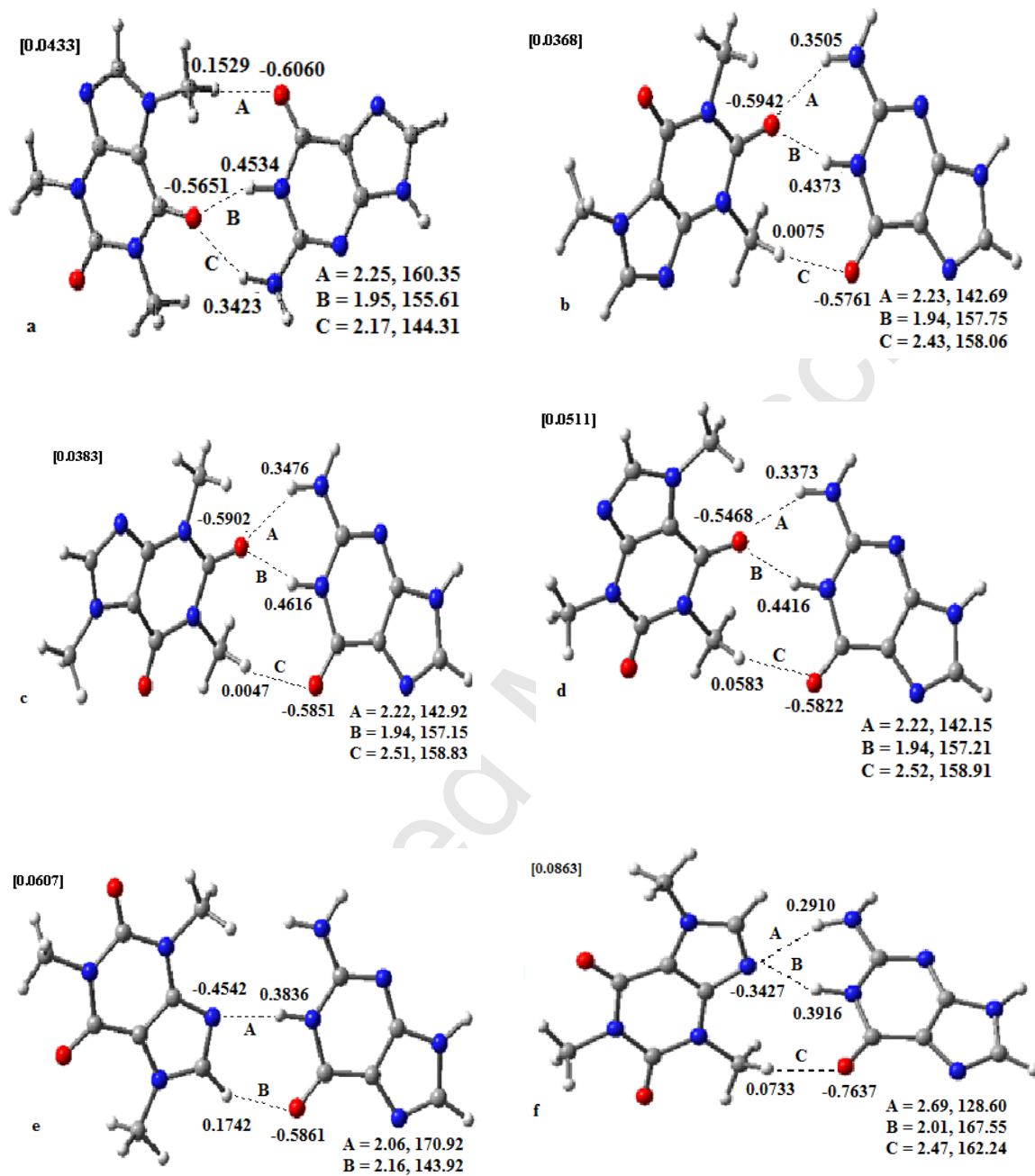


Fig. 2.

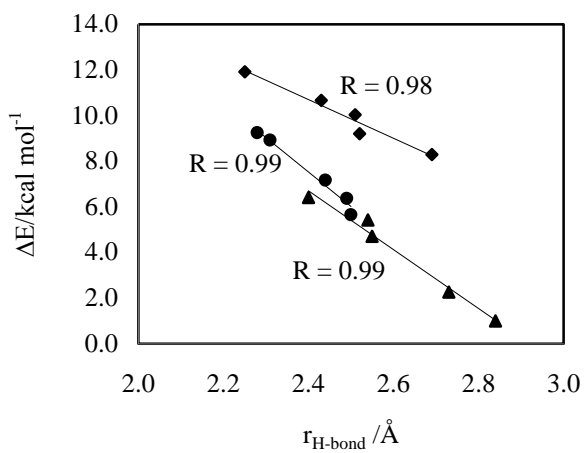


Fig. 3.

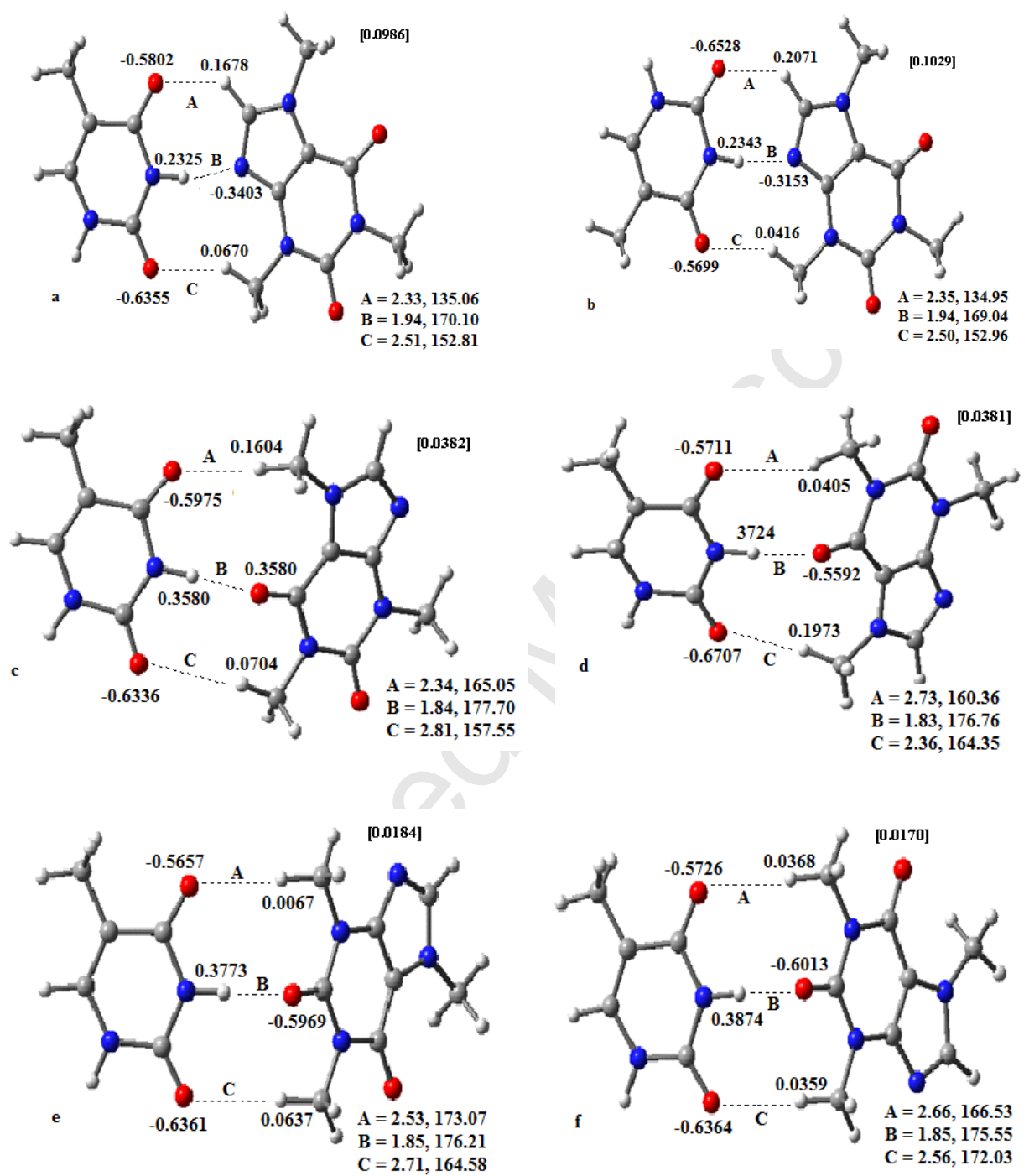


Fig. 4.

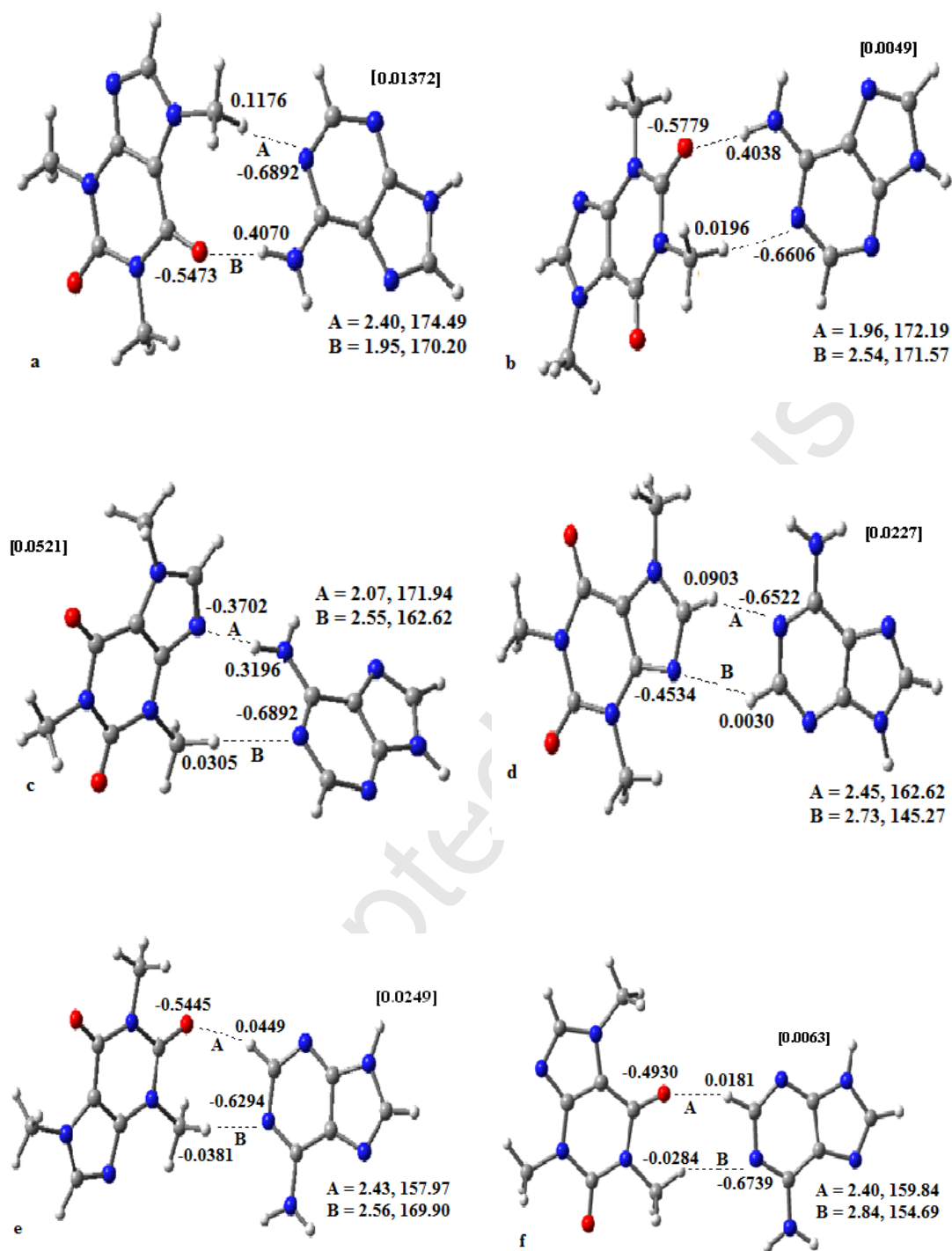


Fig. 5.

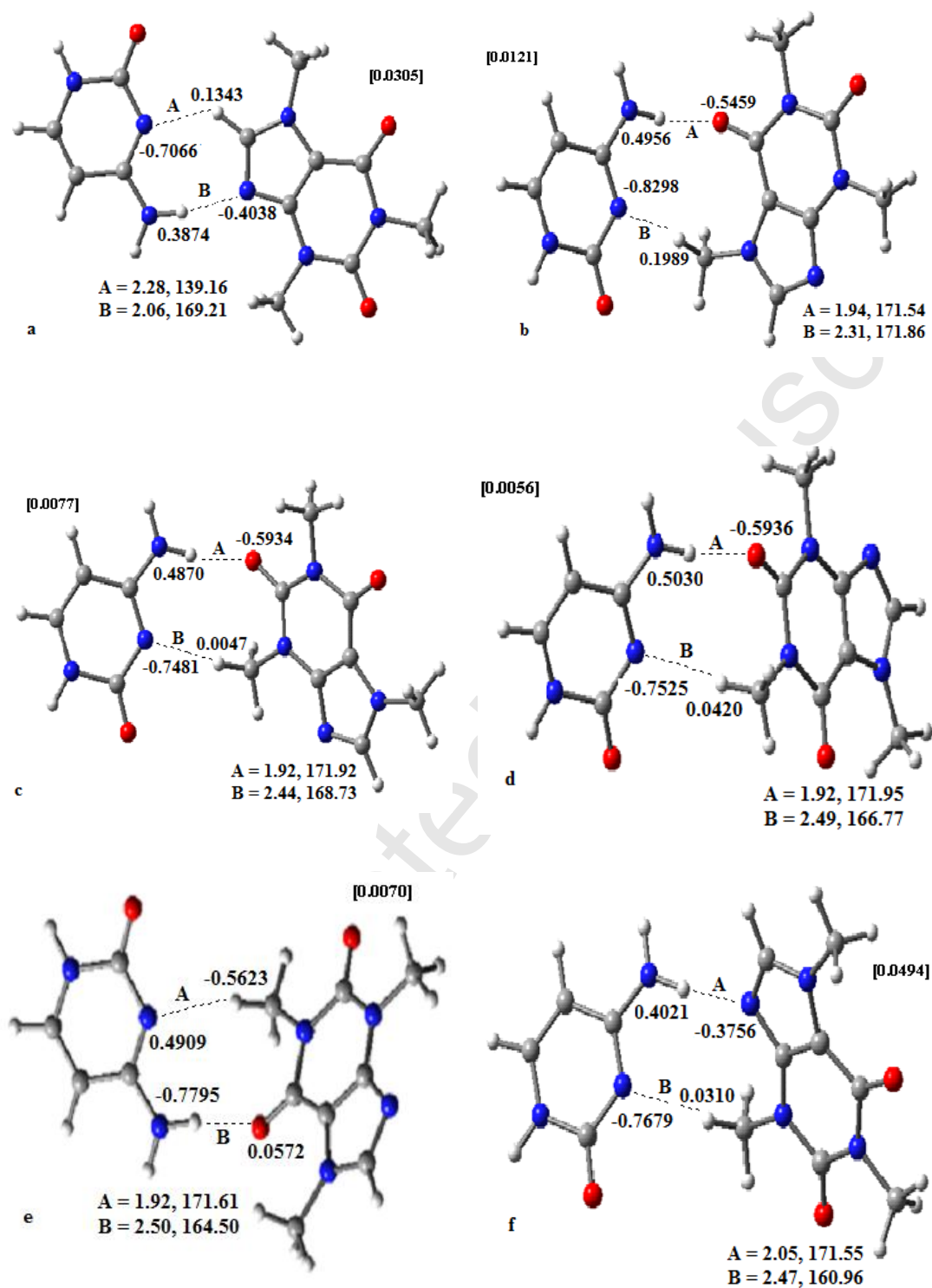


Fig. 6.